

J.T. BONARSKI\*, L. TARKOWSKI\*, S. PAWLAK\*, A. RAKOWSKA\*, Ł. MAJOR\*

## MATERIALS STRESS DIAGNOSTICS BY X-RAY AND ACOUSTIC TECHNIQUES

### DIAGNOSTYKA NAPRĘŻEŃ MATERIAŁÓW PRZY POMOCY TECHNIKI RENTGENOWSKIEJ I AKUSTYCZNEJ

Performed investigations and obtained results concerned the analysis of residual stresses in near-surface areas of copper-corundum ( $\text{Cu-Al}_2\text{O}_3$ ) composite and silicon carbide (SiC) samples. X-ray diffraction and acoustic tomography techniques, as well as the suitable calculation procedures, allowed to locate sample-areas with extreme values of stresses residing in the examined materials. The registered texture-stress characteristics reflects inhomogeneity of the samples structure identified by means of acoustic tomography. Obtained results provide valuable information on anisotropy of physical properties of structural elements produced by the technologies applied to the examined samples.

*Keywords:* metal-matrix composite, residual stresses, crystallographic texture, acoustic microscopy

Przeprowadzone badania i uzyskane wyniki dotyczyły analizy naprężeń w pobliżu obszarów powierzchniowych dwóch typów materiałów: kompozytów  $\text{Cu-Al}_2\text{O}_3$  oraz węgla krzemu (SiC). Do zlokalizowania obszarów skrajnych wartości naprężeń w badanych materiałach użyto dwóch technik dyfrakcji rentgenowskiej i tomografii akustycznej wykorzystując skaningowy mikroskop akustyczny. Zarejestrowana tekstura krystalograficzna oraz naprężenia własne odzwierciedlają niejednorodność próbek zidentyfikowaną za pomocą tomografii akustycznej. Uzyskane wyniki stanowią cenne informacje na temat anizotropii właściwości fizycznych elementów konstrukcyjnych.

#### 1. Introduction

One of the aspects of the intensive development of transport sector (automotive and aviation branches) is aimed – among the others – to increase the power/weight ratio for vehicles driven by internal combustion engines. Progress in the design and construction of the engines and car/plane bodies depends strongly on structural materials. Advanced materials allow to reduce the vehicle mass, while keeping the strength and costs of exploitation at least at the same levels.

One of the solutions in this respect consists in application of aluminum alloys that are much lighter than steel, yet much more plastic at similar strength. Another increasingly popular material-related solution in the mentioned field is to apply metal-matrix-composites (MMC) [1]. They are characterized by higher hardness and high temperature stability as compared to alloys they would substitute. Novel MMC and metal-ceramic functionally-graded materials (FGMs) combining high strength of alloys with ceramic wear resistance offer properties that predispose them for exhaust and propulsion systems, power transmission systems, and braking systems [2].

Copper-corundum coatings ( $\text{Cu-Al}_2\text{O}_3$ ) deposited on metallic substrate seem to be one of more promising material solutions that can be applied in thruster systems. However, a new production technology of this material is still to be found, which overcame a significant difference in the values of the

thermal expansion coefficient of Cu and  $\text{Al}_2\text{O}_3$  as well as the tendency of corundum powder to agglomerate [3, 4].

The residual stresses are very sensitive microstructure characteristics to the actual condition of the material and help to assess its tendency to deteriorate in working conditions. Recognizing the stress distribution in the near-surface layer (like the above-mentioned  $\text{Cu-Al}_2\text{O}_3$  coatings) and its configuration in the bulk of defined structural component (like SiC plates applied in an aerospace- and military industry) are very useful. The stresses in the near-surface layer can be identified by means of traditional X-ray diffraction technique. The bulk stresses configuration can also be identified with the scanning acoustic microscopy [5]. The technique based on relation between a sound velocity and elastic properties (Young modulus) of material allow revealing a depth-profile of elastic inhomogeneity, and the same – to some extent – configuration of field of the residual stresses.

As far as existing methods of material research based on X-ray technique refer to macro- or meso-scale, modern sources of this radiation (e.g. high-energy photon beam) available at present allow to analyse the structure of construction in elements micro- or sub-micro scale. Furthermore, the completely non-invasive measurement method by means of a synchrotron beam makes it also possible to get information on the 3-D organization of crystallites (texture) or the distribution of residual stresses with relatively high spatial resolution. By means

\* INSTITUTE OF METALLURGY AND MATERIALS SCIENCE OF THE POLISH ACADEMY OF SCIENCE, REYMONTA 25 STR., 30-059 KRAKÓW, POLAND

of the scanning acoustic microscopy, it is possible to follow the range of the stress field in the bulk of materials.

The above-mentioned techniques (X-ray diffraction and acoustic microscopy) were applied in the investigation of stress-texture characteristics of exemplary selected materials with different structure and properties: the metal-matrix composite (Cu-Al<sub>2</sub>O<sub>3</sub>) and ceramic (SiC) samples in the form of cuboids. The investigation was aimed at attempting to answer the following questions:

- to what extent does the stresses existed in the near-surface area reveal the bulk configuration of the characteristics?
- is the texture of deposited coating an essential material feature for the residual stress distribution?

## 2. Materials and methods

The exemplary selected CMM-type material (Cu-Al<sub>2</sub>O<sub>3</sub>) and ceramic-type one (SiC) were examined:

Cu-Al<sub>2</sub>O<sub>3</sub> – with 2% vol. and 10% vol. of ceramic phase, deposited on Cu-discs (Ø25 mm, thickness: 4 mm) by the spray technology (denoted as the “cold” process) or by the High Velocity Oxygen Flame spraying (HVOF) (denoted as the “hot” process). The material was manufactured by EDAS IW (Germany). Sample density varied in the range of 8.86÷8.46 g/cm<sup>3</sup>, depending on the contents of corundum with the grain size of 10÷45 μm.

SiC (silicon carbide) – with hexagonal lattice ( $a_0 = 3.0810 \text{ \AA}$ ,  $c_0 = 10.0610 \text{ \AA}$ ,  $\alpha = 90^\circ$ ,  $\beta = 90^\circ$ ,  $\gamma = 120^\circ$ ) [6], fabricated in consolidation and sintering processes carried out at the Institute of Ceramics and Building Materials, Warsaw (Poland). The SiC samples were represented by two plates (50×50×10 mm<sup>3</sup>): the first prepared traditionally through consolidation and sintering, the second one in the High Isostatic Pressure (HIP) process (at the pressure of 3000 bars and temperature of ca. 2000°C). The combination of the two parameters (pressure and temperature) provides a ceramic sample with unique optical and mechanical specificity.

The stress and texture analyses of the examined samples of Cu-Al<sub>2</sub>O<sub>3</sub>-coatings and SiC-plates were based on X-ray measurements carried out through application of appropriate methods. The stresses were measured on the singular diffraction profiles ( $311$  for Cu and  $113$  for SiC) by the  $\sin^2\psi$  method [7]. Data processing in the stress analysis was performed by the standard procedure [8] as well as the MAUD one [9]. Next, the texture (of the Cu-Al<sub>2</sub>O<sub>3</sub> only) was analyzed on the basis of a set of incomplete pole figures for Cu-phase registered by the back-reflection Schulz’s method. In the texture analysis, the discrete Arbitrarily Defined Cells (ADC) [10] method was used.

The measurements were carried out on flat sample surfaces by means of filtered radiation of CoK $\alpha$ -series, while the incident beam was 1 mm in diameter. The XRD investigations were preceded by evaluation of microstructure homogeneity of the samples by means of the acoustic scanning microscopy technique with the signal frequency within the range of 15-110 MHz.

## 3. Results and discussion

Microstructure of the cross-sections of investigated Cu-Al<sub>2</sub>O<sub>3</sub> coatings revealed using scanning electron microscopy technique is shown in Fig. 1. The thickness of Cu-Al<sub>2</sub>O<sub>3</sub> coatings was varied from 70 to 170 μm and the surface of Cu/Cu-Al<sub>2</sub>O<sub>3</sub> interfaces is strongly undulated. The rough substrate surface helps to improve coatings adhesion. The next observation concerns the presence of voids in the interface region, which seem to be larger and appear more frequently in the samples processed by means of the cold technology as compared to the hot-processed ones. Microstructure imperfections can play the role of disadvantageous concentrators of stresses in working conditions.

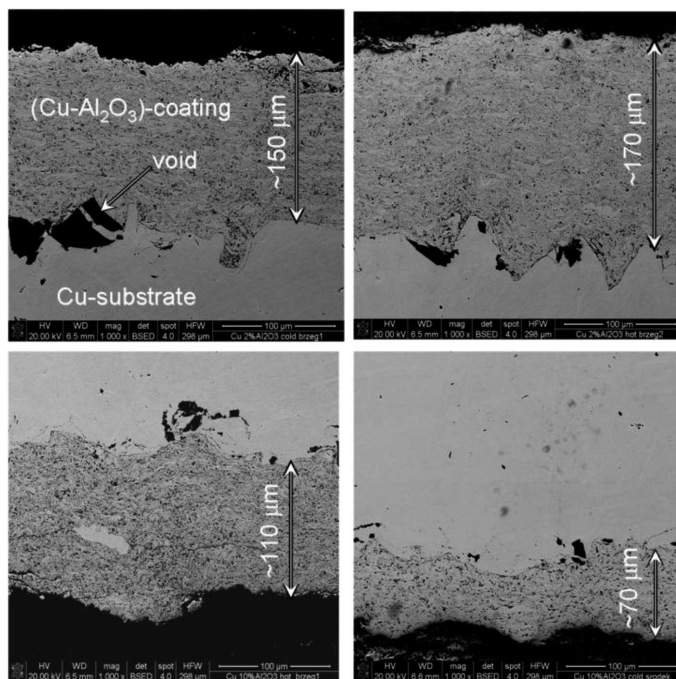


Fig. 1. Microstructure of Cu-Al<sub>2</sub>O<sub>3</sub> coatings containing 2% vol. (top) and 10% vol. (bottom) phases of ceramic deposited on Cu-substrate by the cold- (left) and hot technology (right), the scale marker shows distance of 100 μm

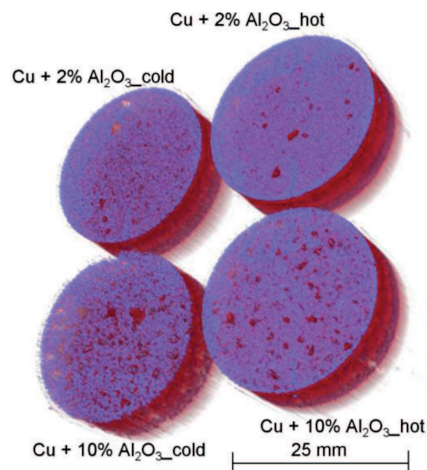


Fig. 2. Spatial inhomogeneity of the elastic properties of the examined samples identified by means of the scanning acoustic microscopy technique (blue- and dark color correspond to the acoustic response of the coatings and substrate, respectively)

Microstructure of the samples revealed by the scanning acoustic microscopy (SAM) technique given in Fig. 2 indicated presence of areas with strongly inhomogeneous elastic properties. The resultant acousto-graphs (processed by dedicated software [11]) show spatial distribution of selected sample areas with different ability to scattering the ultrasound waves. The darker spots (Fig. 2) randomly distributed throughout the Cu-Al<sub>2</sub>O<sub>3</sub> coatings indicate material with less density due to, for instance, a higher concentration of pores.

**Texture** of the Cu-substrate as well as Cu-phase in the individual Cu-Al<sub>2</sub>O<sub>3</sub> coatings in form of the complete (111)-pole figures are presented in Fig. 3. The texture development in the examined materials can be ascribed to the weaker ones. However, it exhibits a tendency to increase in the case of the samples processed by means of the hot technology. As it can be noticed, the pole figure of the substrate indicates the presence of the cold rolling texture of Cu, the real rolling direction (RD) of which is rotated in the sample plane by ca 30° with reference to the marked one. The pole figures of individual coatings exhibit a tendency to form <001>-axial-type texture with traces of the component identified also in the texture of the substrate. This can be the result of the texture inheritance effect, the intensity of which is the strongest in the coatings containing 10% of the Al<sub>2</sub>O<sub>3</sub> phase, irrespective of the applied technology. In that case, the thickness of the deposit is relatively the smallest one and, for that reason, the inheritance effect is the most distinct. On the other hand, it seems that the cold technology favors the formation of axial-type of texture, irrespective of the addition of the corundum phase.

**Residual stresses** of the examined samples (Cu-Al<sub>2</sub>O<sub>3</sub>-coatings and SiC-plates) were analyzed for larger areas of their outer surfaces in a topographic mode with 5×5 mm grid. 2D maps of the stresses in one selected plane (perpendicular to the sample surface) are presented in Fig. 4. Numerical values of the stresses for Cu-phase only in the case of Cu-Al<sub>2</sub>O<sub>3</sub> coatings were calculated regarding the elastic constants by Reuss model [8,12] using the STRESSFIT software package based on the model developed by Baczmański et al. [13]. In the case of SiC plates, suitable calculations were carried-out by the MAUD's procedures [9]. The values of the stiffness  $c_{ij}$  and compliance  $s_{ij}$  tensors used in the

stress calculations for examined materials are given in Tab. 1. [14,15].

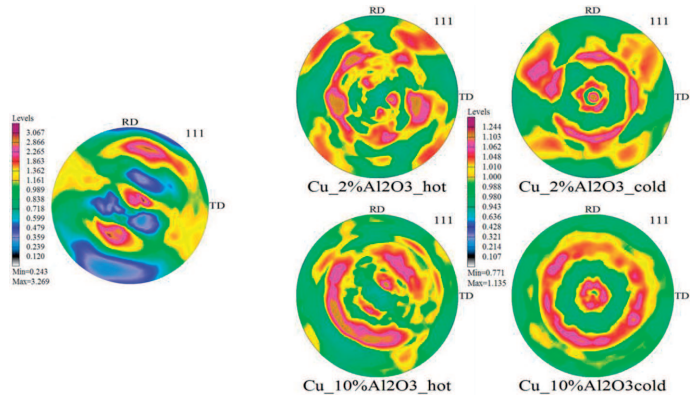


Fig. 3. Crystallographic texture of the near-surface layer of the substrate (left) and the Cu-Al<sub>2</sub>O<sub>3</sub> coatings (right) presented in form of the complete (111)-pole figures of Cu phase

The planar distribution of stresses in Cu-phase identified for the examined Cu-Al<sub>2</sub>O<sub>3</sub> coatings (given in Fig. 4) reveal its higher averaged values for samples processed by the hot technology, in comparison to the samples after the cold process. The stresses distribution seems to be more homogeneous in the coatings with a 2% admixture of Al<sub>2</sub>O<sub>3</sub>. The observed differences in the topography of stresses reflect the conditions of the consolidation process of individual samples.

In the case of SiC samples, the identified stress distribution is essentially different from sample to sample and corresponds to some extent to the internal configuration of the elastic properties of the samples, revealed by the scanning acoustics microscopy technique (Fig. 5). Locations of the sample areas with extreme values of the residual stresses identified by XRD method are given in the 2D stress maps. The applied acoustic tomography made it possible to estimate microstructure inhomogeneity with the spatial resolution of ca. 30 μm. The projection of the bulk inhomogeneity of material elasticity (differentiated Young modulus) in topography of the stress identified by XRD technique is much more distinct for the SiC sample manufactured by means of the HIP technology in comparison to the traditional one.

TABLE 1

Values of the compliance  $c_{ij}$  and stiffness  $s_{ij}$  tensors used in calculation of residual stresses for the examined materials (stresses for the  $\alpha$ -Al<sub>2</sub>O<sub>3</sub>-phase are not presented in the work)

Cu				$\alpha$ -Al <sub>2</sub> O <sub>3</sub>				SiC			
$c_{ij}$	GPa	$s_{ij}$	GPa <sup>-1</sup>	$c_{ij}$	GPa	$s_{ij}$	GPa <sup>-1</sup>	$c_{ij}$	GPa	$s_{ij}$	GPa <sup>-1</sup>
$c_{11}$	0.00017	$s_{11}$	0.01289	$c_{11}$	497	$s_{11}$	0.00235	$c_{11}$	501	$s_{11}$	0.00210
$c_{12}$	0.00011	$s_{12}$	-0.00519	$c_{12}$	163	$s_{12}$	-0.00070	$c_{12}$	111	$s_{12}$	-0.00044
$c_{13}$	0.00011	$s_{13}$	-0.00519	$c_{13}$	116	$s_{13}$	-0.00038	$c_{13}$	52	$s_{13}$	-0.00011
$c_{14}$	0.00000	$s_{14}$	0.00000	$c_{14}$	22	$s_{14}$	-0.00048	$c_{14}$	0	$s_{14}$	0.00000
$c_{33}$	0.00017	$s_{33}$	0.01289	$c_{33}$	501	$s_{33}$	0.00216	$c_{33}$	553	$s_{33}$	0.00189
$c_{44}$	0.00006	$s_{44}$	0.01639	$c_{44}$	147	$s_{44}$	0.00690	$c_{44}$	163	$s_{44}$	0.00614

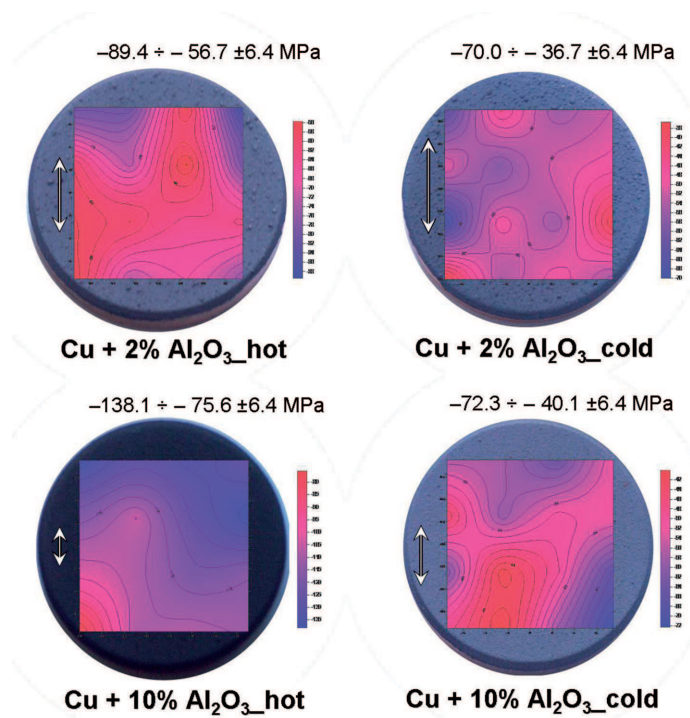


Fig. 4. Topography of residual stresses of Cu-phase in the near-surface layer in the Cu-Al<sub>2</sub>O<sub>3</sub> coatings identified by X-ray diffraction technique in direction marked by the arrows

The reason is a relatively simple, conical-like shape of the bulk-space configuration of elastic inhomogeneity observed in the 3D acousto-graph prepared for the sample (see Fig. 5). Such a simple spatial configuration of the elastic properties was not observed for the SiC sample prepared by means of the traditional technology.

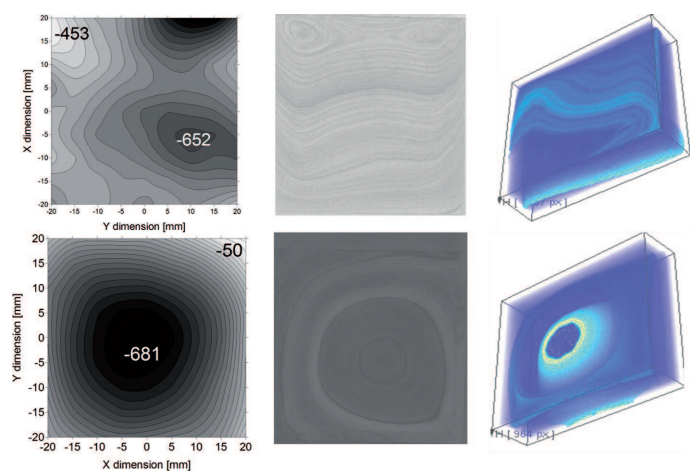


Fig. 5. Planar distribution of residual stresses (left column) in the SiC plates manufactured by traditional (top row) and HIP (bottom row) technology identified by XRD technique, and the 2D- (middle column) and 3D (right column) acoustic images related to the samples

#### 4. Summary

The usefulness of the stress topography in diagnosing the state of microstructure has been verified. Obtained results provide valuable information on anisotropy of physical properties

of structural elements produced by the technologies applied to the examined samples.

The results obtained by the XRD- and acoustic techniques allowed the Cu-Al<sub>2</sub>O<sub>3</sub>-coatings microstructure to be characterized in macro- and microscale. The identified inhomogeneities of the coating morphology have an impact on their working properties. Diversified thickness and production technology of the coatings influence their texture of Cu-component which, to some extent, is moderated by the orientation-inheritance effect. The stresses in the near-surface layer seem to be more insensitive when texture of the layer shows a tendency to crystallographic relations with the substrate. The production technology plays the crucial role for stress distribution in the examined MMC material. Regarding the above characteristics of morphology and identified texture and stress distribution, the coatings with Cu+10%Al<sub>2</sub>O<sub>3</sub> appear to be a potentially better structural material, for instance for thruster applications, than the Cu+2%Al<sub>2</sub>O<sub>3</sub> ones and the hot technology is preferable.

In the case of SiC samples, the location areas with extreme values of the residual stresses identified by the XRD method corresponds to the area indicated by the acoustic tomography (Fig. 5). A good correspondence between the two types of results is noticeable, especially in the case of the SiC sample manufactured by the HIP technology. Such a multi-scale analysis is advantageous in the case of ceramic- or metal-ceramic materials, where a significant inhomogeneity of microstructure is expected.

The presented results of stress topography and texture of the examined plates show how to obtain valuable characteristics of microstructure and how to learn more about the specificity of materials. The calculated values of residual stresses indicate that the stresses are mostly of compressive character in both Cu-Al<sub>2</sub>O<sub>3</sub> and SiC samples.

The described investigations also provide an affirmative answer to the questions posed in the introduction concerned to correspondence between residual stresses (and texture) in the near-surface layer of the construction elements and a state of their microstructure. The relation is clearly visible, particularly in the SiC-plates formed by the HIP technology.

#### Acknowledgements

The results presented in this paper have been obtained within the project "Micro- and Nanocrystalline Functionally Graded Materials for Transport Applications" MATTRANS (grant agreement no. 228869 with the European Union) in the Seventh Framework Programme, as well as project N N507 303540 supported by the National Science Centre (NCN).

#### REFERENCES

- [1] T.W. Clyne, P.J. Withers, An Introduction to Metal Matrix Composites (Cambridge University Press, Cambridge 1993).
- [2] J. Sobczak, S. Wojciechowski, Współczesne tendencje praktycznego zastosowania kompozytów metalowych. *Kompozyty (Composites)* 2, 3, 24-37 (2002).
- [3] H. Gul, F. Kilic, S. Aslan, A. Alp, H. Akbulut, Characteristics of electro-co-deposited Ni-Al<sub>2</sub>O<sub>3</sub> nano-particle

- reinforced metal matrix composite (MMC) coatings, *Wear* **267**, 976-990 (2009).
- [4] L. Du, B. Xu, S. Dong, H. Yang, X. Wu, Preparation, microstructure and tribological properties of nano-Al<sub>2</sub>O<sub>3</sub>/Ni brush plated composite coatings, *Surface & Coatings Technology* **192**, 311-316 (2005).
- [5] Crystallographic Database ICDD, PDF+4 package (2010).
- [6] I.C. Noyan, J.B. Cohen, *Residual Stresses – Measurement by Diffraction and Interpretation* (Springer-Verlag, Berlin 1987).
- [7] N.G.H. Mayendorf, P.B. Nagy, S.I. Rokhlin, *Nondestructive Materials Characterization with application to Aerospace Materials* (Springer-Verlag, Berlin, Heidelberg 2004).
- [8] A. Baczmański, *Stress field in polycrystalline materials studied using diffraction and self-consistent modeling* (Thesis, AGH UST, Kraków 2005).
- [9] L. Lutterotti, P. Scardi, Simultaneous Structure and Size-Strain Refinement by the Rietveld Method, *J. Appl. Cryst.* **23**, 246-252 (1990).
- [10] K. Pawlik, Determination of the orientation distribution from pole figures in arbitrarily defined cells. *Physica Stat Solidi (B)* **134**, 477-483 (1986).
- [11] K. Kudłacz, Computer program SAM3D (IMIM PAN, Kraków 2009).
- [12] A. Reuss, Berechnung der Fließgrenze von Mischkristallen auf Grund der Plastizitätsbedingung für Einkristalle, *A. Angew. Math. Mech.* **9**, 49 (1929).
- [13] A. Baczmański, K. Wierzbowski, J. Tarasiuk, Models of plastic deformation used for internal stress measurements, *Zeitschrift fuer Metallkunde/Materials Research and Advanced Techniques* **86**, 7, 507-511 (1995).
- [14] D.B. Hovis, A. Reddy, A.H. Heuer, X-ray elastic constants for Al<sub>2</sub>O<sub>3</sub>, *Appl. Phys. Lett.* **88**, 131910-131913 (2006).
- [15] <http://133.1.55.10/Cij.database/>